Improving Efficiency of Human-Robot Coexistence while Guaranteeing Safety: Theory and User Study

Aaron Pereira[1], *Non-Member, IEEE,* Mareike Baumann[2], *Non-Member, IEEE,* Jonas Gerstner[2], *Non-Member, IEEE,* Matthias Althoff[2] *Member, IEEE,*

Abstract—Guaranteeing safety for humans in shared workspaces is not trivial. Not only must all possible situations be provably safe, but the human must *feel* safe as well. While robots are gradually leaving their cages, due to strict safety requirements, engineers often only replace physical cages with static safety zones—when the safety zone is entered, the robot is forced to stop. This can lead to excessive robot downtime.

We present a concept for guaranteeing non-collision between humans and robots whilst maximising robot uptime and staying on-path. We evaluate how users react to this approach, in a trial over three non-consecutive days, compared to a control approach of static safety zones. We measure working efficiency as well as human factors such as trust, understanding of the robot, and perceived safety. Using our approach, the robot is indeed more efficient compared to static safety zones and the effect persists over multiple trials on separate days. We also observed that understanding of the robot's movement increased for our method over the course of trials, and the perceived safety of the robot increased for both our method and the control.

Note to Practitioners—We describe an ISO-standard-compliant approach for allowing robots to operate safely in areas where human workers frequently enter. Instead of the robot having to stop when the worker enters the workspace, the robot can slow such that it is always able to stop before the worker comes into contact. This safety control can be implemented in parallel to existing control and trajectory planning. We conducted tests over multiple days, so that users had a chance to get used to the robot. We found that our approach allowed the robot to work with **36%** less stoppage time. We also saw that the workers felt safer after multiple trials with the robot, and also (for our method) gained a better understanding of the robots movement. Any sensor, such as a camera, can be used to track the position of the worker, but for these tests we used a motion-capture system.

Index Terms—Safe Human-Robot Coexistence, Human Factors, Formal Verification

I. INTRODUCTION

AS use cases for robots working in human workspaces increase, not only on the production line but in warehouses, the service industry and elsewhere, humans may often need to safely enter the robot's workspace to grab a tool, to complete a task near the robot (where space is restricted), or may simply enter by accident. Guaranteeing their safety—while allowing the robot to work efficiently—is a key concern for those wishing to introduce robots to their enterprises [1].

Following ISO 10218-1 [2], four modes for robot control in shared workspaces are allowed:

[1] German Aerospace Center, Münchener Str. 20, 82234 Weßling, Germany Corresponding e-mail: aaron.pereira@dlr.de
[2] Fakultät für Informatik, Technische Universität München, Boltzmannstr. 3, 85748 Garching, Germany

1) **Safety-rated monitored stop (SRMS)**—Robot performs a controlled stop when a human enters the (collaborative) workspace, resuming when the human leaves.
2) **Hand guiding**—A hand-held and hand-operated device is used to transmit motion commands to the robot.
3) **Speed and separation monitoring (SSM)**—Humans are allowed in the robot's workspace, but the robot limits its speed and its distance to them.
4) **Power and force limiting**—The robot's power and potential impact force are limited to ameliorate severity in case of impact.

Where robots operate autonomously (i.e. not hand-guided) and should not permit collisions while in motion (due to e.g. a risk of clamping, high inertia robots which cannot stop fast enough, or lack of collision-sensing), two options remain: SRMS and SSM. The latter is expected to be more efficient, since robots can work despite humans in the workspace.

A. Safe trajectory planning in human-robot co-existence

Robots in shared workspaces must account for nearby humans and their immediate motion, but predicting this motion is a challenge. Predictor models such as Gaussian mixture models [3], hidden Markov models [4], or other learning algorithms [5], [6] have been used to estimate most likely motion from initial movement. To be fully safe, however, we must account for *all* possible movement. In previous work [7] we proposed a method for formally-verified speed and separation monitoring (VSSM), based on the framework of partial motion planning [8], using a set-based prediction of human motion. The robot continually verifies each increment of motion against safety criteria before executing it, and accordingly updates its trajectory, without deviating from the predefined path of the original trajectory. We expect this method to be more efficient than SRMS, but this must be tested experimentally. Furthermore, purely mathematical arguments will not convince those who work with the robot. Do workers understand how the robot reacts to them? Do they work faster or slower with VSSM or SRMS? Do they feel safe? We are therefore also interested in the human reaction—especially after the novelty of the first encounter has worn off.

B. Trust and perceived safety

A well-engaged workforce comfortable working alongside robots is not only beneficial for reasons of productivity, but also on ethical grounds. This is referred to in [9] as *psychological safety*. Akalin et al. [10] found that perceived safety in

human-robot interaction (HRI) correlates with users' comfort, sense of control, and trust, when working with a robot that was sometimes faulty, but that personality (e.g. neuroticism) played a role. Trust of the developers alone may not be enough to inspire trust in its systems, since Jensen *et al.* [11] found that the system and its developers are perceived as distinct when assigning blame related to trust of the system. You et al. [12] found that perceived safety increases users' intention to work with the robot in virtual reality (VR). Users wore a head-mounted display and their movements were tracked and mapped to an avatar in VR. They also found that separating working areas with a fence increases perceived safety.

A number of factors affect how much humans trust robots. Hancock *et al.* [13] divide these into factors related to the human (learned abilities and personality), to the robot (its performance, anthropomorphism, proximity) and to the environment. The robot's performance was found to have a large effect on trust; human-related factors had a smaller effect. Rossi *et al.* [14] found that the loss of trust caused by system errors depends on timing and magnitude of these errors. Attempts have been made to model (experiential) trust [15]. Trust could thus be built into algorithms for robot control, e.g. in [16], where a optimal trajectory planner uses a measure of trust in its cost function, or in [17], where the control regime of the robot is switched depending on the level of trust.

C. User studies of adaptation to robots

In industrial human-robot coexistence or in service robotics, workers may not have prior experience with robots—their first impressions towards their robotic co-workers may change as they grow accustomed to them. However, the sheer novelty of HRI experiments can often lead to unrepresentative responses from participants in terms of trust and reported safety [18].

Longer-term studies of HRI have focussed on service robotics [19]–[21], rehabilitation [22], or automated driving and teleoperation of unmanned vehicles [23], [24]. Industrial human-robot coexistence suffers from an absence of such research [25]. In most studies subjects encounter the robot physically only once (e.g. [26], [27]) or not at all. In the latter cases, the subject only observes recorded behaviour of the robot (e.g. [28], [29]). The less contact with the robot, the less the study can reveal about co-working after the initial encounter, making it less relevant to real co-working situations.

In [30], habituation to robots' approach distances and directions was observed after the second independent encounter. In our own previous experiments [31], users commented that their perceptions towards the robot changed after a few trials with the robot. In [32], 60 trials were distributed over three days and even in the first few trials improvement in operator performance and trust was found. Based on this precedent, we also spread the trials over three (non-consecutive) days.

D. Paper Structure and Contributions

This paper presents and evaluates an approach to formally-verified speed and separation monitoring (VSSM). The approach is an interplay of trajectory planning and set-based prediction. The following two sections describe in detail how

the robot plans and verifies its path subject to constraints on joint acceleration and jerk, and accounting for sensor and system latency, such that it guarantees safety to surrounding humans. A version of this planning was presented in [7]; in Sec. II we generalise the approach, discuss shortcomings of the method, and how to deal with these shortcomings. In Sec. III, we describe how sets of human and robot future occupancy are predicted efficiently to feed into the trajectory planning.

We conducted a multi-day user study—to the authors' knowledge, the first detailed user study of a formally correct SSM approach accounting for system latency. We tested whether VSSM is indeed more efficient than SRMS (result first reported in [33]) but crucially, how both approaches are experienced by the human co-worker, and how this changes with experience with the robot. Specifically, we see how their understanding of the robot's motion, attitude towards the developers and perception of safety change with experience with the robot. We also show that after experience with the robot, differences in perceived safety can be observed which cannot be observed after only one interaction. This lends weight to the postulation that observations from initial interaction with a robot cannot give a reliable image of continued interaction. We present the investigation in Sec. IV, evaluate our hypotheses in Sec. VI, discuss findings in Sec. VI, and present our conclusions in Sec. VII.

II. FORMALLY-VERIFIED SPEED AND SEPARATION MONITORING (VSSM)

Our approach is based on the principle that *no action is carried out, until it is verified safe*. While following a desired trajectory[1] in joint space, the robot has at all times a *failsafe manoeuvre* at its disposal that will bring it to a safe state before the human can reach it. The concept is shown in Fig. 1; t_0, t_1 and t_2 are successive time points one cycle-time apart. Prior to time t_0, the robot has verified that it can execute its desired trajectory from t_0 to t_1, followed by a failsafe manoeuvre until $t_{e,1}$, without coming into contact with any human. We call this piece of trajectory plus failsafe manoeuvre the *short-term plan*.

While executing the desired trajectory from t_0 to t_1, the robot verifies the next short-term plan (from t_1 to t_2 followed by a failsafe manoeuvre until $t_{e,2}$) in the same way. If the potential future spatial occupancies (*reachable occupancies*) of the robot and surrounding humans intersect, as is the case in Fig. 1, the robot *might* not be able to reach a safe state before the human reaches it, if it would continue on the desired trajectory after time t_1. Hence, the robot takes the failsafe manoeuvre verified prior to t_0 at time t_1 instead. This would also happen in case a sensor malfunction is detected, or the perception module is not certain that all surrounding humans are detected. While executing the failsafe manoeuvre, the robot plans a *recovery manoeuvre* back to the desired trajectory, and verifies this in the same way as it would the desired trajectory. We now show how to plan the short-term plan in more detail.

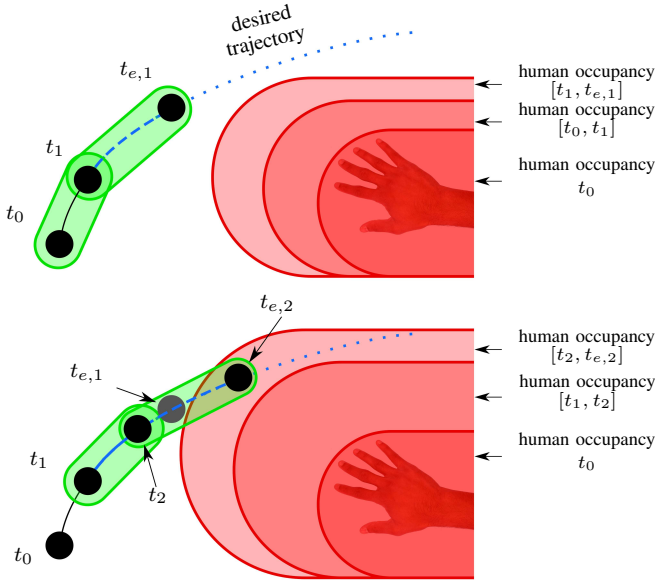[1] A joint space trajectory is formally defined below in Def. 1.

Fig. 1. Above: current short-term plan consisting of desired trajectory until t_1 followed by a failsafe manoeuvre, verified safe prior to t_0. Below: desired trajectory is unsafe after time t_1, since the robot's occupancy during the next short-term plan (green) would intersect the potential future occupancy of the human (red). Failsafe manoeuvres are shown as dashed lines.

A. Planning the Short-Term Plan

The failsafe and recovery manoeuvres are chosen to be path-consistent—only scaling the speed along the desired trajectory subject to limits on joint acceleration and jerk. Trajectory scaling has been used to ensure trajectories conform to limits on torque (e.g. [34], [35]) or estimated impact energy [36].

By scaling the speed of the trajectory along the desired path, we allow adaptation in dynamic environments without costly spatial replanning; this may be more predictable for human operators in the sense that they know where the robot is going to move. Joint jerk limits prevent damage to drives and vibrations in the robot structure which reduce tracking accuracy, and result in smooth movement despite the verifier signal constantly changing between safe and unsafe. Negative speed, i.e. moving backward along the path, is not allowed.

We define the *desired trajectory* $\boldsymbol{\xi}$ as a trajectory parametrised by a time parameter s (vectors are always in bold type) and thrice differentiable in s:

Definition 1 (Trajectory). *In this work, a trajectory is a continuous mapping from a time parameter $s \in [s_0, s_f]$ to a joint position $\boldsymbol{q} \in \mathcal{Q}$ (where $\mathcal{Q} \subseteq \mathbb{R}^m$ is the joint space of a robot with m joints):*

$$\boldsymbol{\xi} : [s_0, s_f] \to \mathcal{Q}$$

By varying $\dot{s} = \frac{\mathrm{d}s}{\mathrm{d}t}$, we can modulate motion on the spatial path of $\boldsymbol{\xi}$ to be as fast or slow as necessary (motion on the desired trajectory has $\dot{s} = 1$). The short-term plan therefore only needs to be described in terms of the time parameter s. We define the short-term plan starting at t_k as a mapping from time t to the time parameter s, i.e. $\Psi : [t_k, \infty] \to [s_k, \infty]$. Thus, the joint position at time t is $\boldsymbol{\xi}(\Psi(t))$. Let us formally define a *time-scaling manoeuvre*:

Definition 2 (Time-scaling manoeuvre). *Let s_a, $\dot{s}_a$ and $\ddot{s}_a$ be the values of s, $\dot{s}$ and $\ddot{s}$ at time t_a, and $\eta \in [0, 1]$. Then a time-scaling manoeuvre starting at t_a is a monotone function $\psi^\eta : [t_a, \infty] \to [s_a, \infty]$ where $\psi^\eta(t_a) = s_a$, $\dot{\psi}^\eta(t_a) = \dot{s}_a$ and $\ddot{\psi}^\eta(t_a) = \ddot{s}_a$, and for all $t \geq t_b$, $\dot{\psi}^\eta(t) = \eta$, for some finite $t_b \geq t_a$. We call t_a the start and t_b the end of the time-scaling manoeuvre.* $\square$

In short, a time-scaling manoeuvre brings the robot to follow its desired trajectory at a fraction η of the speed. The *failsafe manoeuvre* is a time-scaling manoeuvre with $\eta = 0$, and a *recovery manoeuvre* is one with $0 < \eta \leq 1$.

Overviews of the formally-verified speed and separation monitoring (VSSM) and the verification algorithm are shown in Alg. 1 and Alg. 2 respectively. RRO and HRO stand for the *robot* and *human reachable occupancies* respectively. In Alg. 1, the variables are initialised in lines 1–3. The current value of s, $\dot{s}$ and $\ddot{s}$ (represented for legibility in the algorithm as the vector "state", see line 7), together with the desired trajectory $\boldsymbol{\xi}$ and the current timestep k, are required for planning a time-scaling manoeuvre. The VSSM algorithm starts when the robot is stationary, and the first failsafe plan in line 3 does not cause the robot to move.

During subsequent timesteps, we execute the control command from the previously verified short-term plan $\Psi_{current}$ (in line 5), and plan and verify the next short term plan. For reasons explained in Sec. II-B, we can try several recovery manoeuvres: in line 8 we loop over a range of η in descending order, starting from 1 (i.e., trying to recover to the original trajectory), but no less than the current value of $\dot{s}$. The number of values of η depends on the application and the amount of computing power available, but at least $\eta = 1$ must be tried.

If η is the same as that used in the previous step's short-term plan (if it was verified safe in the last timestep), there is no need to plan a new recovery manoeuvre, since the robot is already on this manoeuvre. Otherwise, we plan a recovery manoeuvre ψ^η (line 10). One step along this recovery manoeuvre, we plan a failsafe manoeuvre ψ^0 (line 12). This forms the new short-term plan $\Psi_{proposed}$. Note that, if a human is too far away to be verified unsafe and the robot is moving at $\dot{s} = 1$, the recovery manoeuvre is trivial, i.e. in Def. 2, $t_b = t_a$, $\eta = 1$ and $\dot{\psi}^\eta(t) = 1$ for the entire trajectory. Fig. 2 is a sketch-plot of a short-term plan, showing $\dot{s}$ versus time t.

We then verify the short-term plan as in Alg. 2. We may use one safety criterion (e.g. the robot must be stationary when the human impacts it) or a set of criteria $\mathcal{C}$. Note that the time t_{e,C_κ} after which the robot is safe, which is used as the prediction horizon, may vary for different criteria—see [7] for an example of different safety criteria in use. If it is safe under all criteria, we update the current short-term plan (line 16). Otherwise, if no value of η yields a safe short-term plan, the robot carries on executing the previous short-term plan, eventually bringing it to a stop.

Next, we show in Alg. 3 how to generate failsafe and recovery manoeuvres subject to limited joint jerk and acceleration. In the following analysis, we denote the Euclidean norm of a vector $\boldsymbol{z}$ as $\|\boldsymbol{z}\|$ and $|\boldsymbol{z}|$ returns elementwise the vector of absolute values.

Algorithm 1 Formally Verified Trajectory Planning

Input: desired trajectory $\boldsymbol{\xi}$, safety criteria $\mathcal{C}$, human sensor data including timestamp $\mathcal{H}_{t_h}$
Output: Safe trajectory
1: $k \leftarrow 0$
2: $\eta_k \leftarrow 0$
3: $\Psi_{current} \leftarrow$ stay in safe state
4: **while** not at goal state **do**
5:     execute_control_on_robot($\Psi_{current}, k$)
6:     $\eta_{k+1} \leftarrow 0$
7:     state $\leftarrow [\Psi_{current}(t_k), \dot{\Psi}_{current}(t_k), \ddot{\Psi}_{current}(t_k)]^\top$
8:     **for** $\eta \in \{1, \eta_1, \eta_2, ...\}$ **do**
9:         **if** $\eta \neq \eta_k$ **then**
10:             $\psi^\eta \leftarrow$ manoeuvre(state, $t_k, \boldsymbol{\xi}, \eta$)
11:         state $\leftarrow [\psi^\eta(t_{k+1}), \dot{\psi}^\eta(t_{k+1}), \ddot{\psi}^\eta(t_{k+1})]^\top$
12:         $\psi^0 \leftarrow$ manoeuvre(state, $t_{k+1}, \boldsymbol{\xi}, 0$)
13:         $\Psi_{proposed} \leftarrow \begin{cases} \psi^\eta(t) & t_k \leq t < t_{k+1} \\ \psi^0(t) & t \geq t_{k+1} \end{cases}$
14:         $\text{safe}_{k+1} \leftarrow$ verify($k, \mathcal{C}, \Psi_{proposed}, \mathcal{H}_{t_h}, \boldsymbol{\xi}$)
15:         **if** safe_{k+1} **then**
16:             $\Psi_{current} \leftarrow \Psi_{proposed}$
17:             $\eta_{k+1} \leftarrow \eta$
18:             **break**
19:     $k \leftarrow k + 1$

Algorithm 2 verify

Input: k, safety criteria $\mathcal{C} = \{C_1, \ldots C_K\}$, short-term plan Ψ, timestamped human sensor data $\mathcal{H}_{t_h}$, desired trajectory $\boldsymbol{\xi}$
Output: $is\_safe \in \{0, 1\}$
1: **for** $\kappa = 1 : K$ **do**
2:     Find time t_{e,C_κ} after which robot is safe according to C_κ, while following Ψ
3:     **if** $t_{e,C_\kappa} > t_k$ **then**   // If robot is not already safe
4:         RRO $\leftarrow$ find_robot_reach_occ($\Psi, t_k, t_{e,C_\kappa}, \boldsymbol{\xi}$)
5:         HRO $\leftarrow$ find_human_reach_occ($\mathcal{H}_{t_h}, t_k, t_{e,C_\kappa}$)
6:         **if** RRO $\cap$ HRO $\neq \emptyset$ **then**
7:             **return** FALSE
8: **return** TRUE

Algorithm 3 manoeuvre

Input: Trajectory parameters, i.e. $[s_a, \dot{s}_a, \ddot{s}_a]^\top$, current time t_a, desired trajectory $\boldsymbol{\xi}$, desired end η
Output: time-scaling manoeuvre ψ^η
1: $\Delta t \leftarrow$ controller timestep
2: $iter \leftarrow 0$
3: $s_b' \leftarrow s_a +$ duration_heuristic($s_a, \dot{s}_a, \ddot{s}_a, \boldsymbol{\xi}$)
4: **while** $iter <$ maximum number of iterations **do**
5:     $\dddot{s}_m, \dddot{s}_m \leftarrow$ find_limits($s_a, s_b', \boldsymbol{\xi}, \eta$) // as in eq. 3–6
6:     $\psi^\eta \leftarrow$ plan_traj($\ddot{s}_m, \dddot{s}_m, \dot{s}_a, \ddot{s}_a, \eta, t_a, \Delta t$)
7:     **if** $s_a +$ length(ψ^η) $< s_b'$ **then**
8:         **return**
9:     $iter \leftarrow iter + 1$
10:     $s_b' \leftarrow$ max($s_a +$ length(ψ^η), s_b') $+ \Delta t$
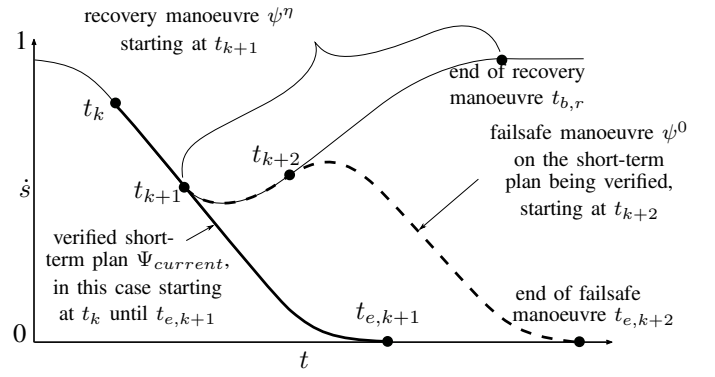   **return**

Fig. 2. Short-term plan: During execution of the verified short-term plan from time t_k to t_{k+1} (bold line), we plan the subsequent short-term plan (dashed bold line), which comprises one step on a recovery manoeuvre (thin line) until t_{k+2}, followed by a new failsafe manoeuvre starting at t_{k+2}.

B. Planning time-scaling manoeuvres with limited acceleration and jerk

To plan the time-scaling manoeuvres (failsafe and recovery), we adapt a method from [37] which finds time-optimal trajectories of joint values $\boldsymbol{q}$ in time, given $\boldsymbol{q}$ and its derivatives at the beginning and end of the trajectory, and subject to limits on derivatives of $\boldsymbol{q}$. Our adaptation uses $\dot{s}$ instead of $\boldsymbol{q}$, and compared to [37], we do not know all parameters a priori: we must first calculate the maximum values of $\ddot{s}$ and $\dddot{s}$ such that the required maximum joint accelerations and jerks are respected. Thus we require:

$$\max_{s \in [s_a, s_b]} (|\ddot{\boldsymbol{\xi}}(s)|) \leq \boldsymbol{a}_{\max}, \tag{1}$$

$$\max_{s \in [s_a, s_b]} (|\dddot{\boldsymbol{\xi}}(s)|) \leq \boldsymbol{j}_{\max}, \tag{2}$$

for certain maximum joint accelerations and jerks $\boldsymbol{a}_{\max}$ and $\boldsymbol{j}_{\max}$ whose values depend on the robot design. Recall from Def. 2 that s_a and s_b are the values of s at the beginning and end of the time-scaling manoeuvre.

1) Case for $\eta = 1$: In [7], we demonstrated that the conditions in (1) and (2) can be satisfied by bounding $\ddot{s}$ and $\dddot{s}$ over the length of the manoeuvre as follows. Let us introduce the vectors $\boldsymbol{\theta}$ and $\boldsymbol{\lambda}$, which are the (elementwise) maximum magnitudes of $\frac{d^2\boldsymbol{\xi}}{ds^2}$ and $\frac{d^3\boldsymbol{\xi}}{ds^3}$ over the portion of the desired trajectory between s_a and s_b. I.e, for each joint i, where ξ_i, θ_i and λ_i are the ith element of $\boldsymbol{\xi}$, $\boldsymbol{\theta}$ and $\boldsymbol{\lambda}$ respectively, then $\theta_i = \max_{s \in [s_a, s_b]} \left(\left| \frac{d^2\xi_i}{ds^2} \right| \right)$ and $\lambda_i = \max_{s \in [s_a, s_b]} \left(\left| \frac{d^3\xi_i}{ds^3} \right| \right)$.

It holds [7, Lemma 1] that $\ddot{\boldsymbol{\xi}}(s) \leq \boldsymbol{a}_{\max}$ and $\dddot{\boldsymbol{\xi}}(s) \leq \boldsymbol{j}_{\max}$ over a scaling manoeuvre starting at s_a and ending before s_b, as long as $|\ddot{s}| \leq \ddot{s}_m$ and $|\dddot{s}| \leq \dddot{s}_m$ over the manoeuvre, where:

$$\ddot{s}_m = \max(\min(\boldsymbol{c}), 0), \quad \boldsymbol{c} = \frac{\boldsymbol{a}_{\max} - \boldsymbol{\theta}}{\left| \frac{d\boldsymbol{\xi}}{ds} |_{s_a} \right| + \boldsymbol{\theta}(s_b - s_a)}, \tag{3}$$

$$\dddot{s}_m = \max(\min(\boldsymbol{d}), 0), \quad \boldsymbol{d} = \frac{\boldsymbol{j}_{\max} - \boldsymbol{\lambda} - 3\boldsymbol{\theta}\ddot{s}_m}{\left| \frac{d\boldsymbol{\xi}}{ds} |_{s_a} \right| + \boldsymbol{\theta}(s_b - s_a)}, \tag{4}$$

and the $\min$ operator takes the minimum element of the vectors $\boldsymbol{c}$ and $\boldsymbol{d}$. We do not know s_b a priori, hence we use a conservative estimate s_b' that we obtain heuristically (line 3 of Alg. 3; if $s_b > s_b'$ after planning the manoeuvre, we

can recalculate with a more conservative estimate of s_b, until $s_b' \geq s_b$.

The manoeuvre is planned in line 6. It is a Type I trajectory from [37], albeit in $\dot{s}$ rather than in $\boldsymbol{q}$. Note—since the trajectory is in $\dot{s}$, "velocity" and "acceleration" in [37] refer to $\ddot{s}$ and $\dddot{s}$. If no manoeuvre is found in time, the control defaults to the previous failsafe trajectory. This is lines 7-10.

2) Case for $\eta < 1$: If $\boldsymbol{\theta}$ and $\boldsymbol{\lambda} + 3\boldsymbol{\theta}\ddot{s}_m$ are close in value to $\boldsymbol{a}_{\max}$ and $\boldsymbol{j}_{\max}$ respectively, the time scaling manoeuvre may be long, and calculating s_b' would need many iterations, or may even be impossible (e.g. if $\ddot{s}_m = 0$ or $\dddot{s}_m = 0$).

This may present problems in industrial scenarios, where the joint accelerations and torques on the desired trajectory may be close to the maximum allowed. Instead, if we plan a recovery manoeuvre to a final value of $\eta < 1$, and enforce $\dot{s} \leq \eta$ throughout this manoeuvre, $\boldsymbol{c}$ and $\boldsymbol{d}$ in equations (3) and (4) become:

$$\boldsymbol{c} = \frac{\boldsymbol{j}_{\max} - \eta^2\boldsymbol{\theta}}{\left|\frac{\mathrm{d}\boldsymbol{\xi}}{\mathrm{d}s}|_{s_a}\right| + \boldsymbol{\theta}(s_b - s_a)}, \tag{5}$$

$$\boldsymbol{d} = \frac{\boldsymbol{j}_{\max} - \eta^3\boldsymbol{\lambda} - 3\eta\boldsymbol{\theta}\ddot{s}_m}{\left|\frac{\mathrm{d}\boldsymbol{\xi}}{\mathrm{d}s}|_{s_a}\right| + \boldsymbol{\theta}(s_b - s_a)}. \tag{6}$$

The derivation of the more general case follows straightforwardly from the proof of [7, Thm. 1], when substituting $|\dot{s}| \leq \eta$. Hence planning a recovery manoeuvre to a smaller η may work where planning to recover to $\eta = 1$ may fail.

If the extrema of $\frac{\mathrm{d}^2\boldsymbol{\xi}}{\mathrm{d}s^2}$ and $\frac{\mathrm{d}^3\boldsymbol{\xi}}{\mathrm{d}s^3}$ can be analytically calculated (e.g. as in a joint-space point-to-point trajectory where position is a polynomial function of the s), finding $\boldsymbol{\lambda}$ or $\boldsymbol{\theta}$ is straightforward. Otherwise, the extrema can be calculated over the entire desired trajectory after it is planned (as we did in Sec. IV).

With these bounds on $|\dddot{s}|$ and $|\ddot{s}|$, it remains to apply the method from [37] to generate a failsafe or recovery manoeuvre in $\dot{s}$ subject to the constraints that $\dddot{s} = 0$ and $\dot{s} = \eta$ ($\eta > 0$ for recovery, $\eta = 0$ for failsafe) at the end of the manoeuvre, that $0 \leq \dot{s} \leq \eta$ during the manoeuvre, and that the second and third derivatives of the trajectory parameter s are bounded, i.e. $|\ddot{s}| \leq \ddot{s}_m$ and $|\dddot{s}| \leq \dddot{s}_m$.

C. Observed behaviour of the robot

The robot moderates its speed to the maximum allowable to allow it to reach a safe state in time. When the human is far away, it works at full speed; when very close, it stops outright. When fairly close, the robot works at a reduced speed, as it alternately verifies the recovery trajectory safe and unsafe. The lower the maximum allowed joint accelerations $\boldsymbol{a}$ and jerks $\boldsymbol{j}$, the smoother the robot's movement, but the more conservative the robot (since time-scaling manoeuvres are longer).

III. OVERAPPROXIMATIVE OCCUPANCY PREDICTION

The predicted occupancy of the human and the future occupancy of the robot, which are required for VSSM behaviour, must be *overapproximative*. That is, they enclose the entire possible spatial occupancy of the human or the robot during the given time interval: only then can the guarantees of noncollision hold, as described in Sec. II. Both occupancies are determined as sets of *capsules* (defined formally below), for which collision checks are fast and deterministic in time (compared to, e.g. collision checks between polyhedra). Hard real time is therefore possible with a fast cycle time. The method to determine robot occupancy is first described in [7]. We recapitulate it here both for completeness, and in order to give the proof of minimal enclosure of two spheres by another sphere or a capsule. It has linear complexity in degrees of freedom (DoFs) of the robot and is a good compromise of computation time and accuracy, compared to, e.g., more complex sphere-swept volumes [38].

A. Ball and Capsule Enclosure

We introduce first some operators and terminology. All norms are Euclidean.

Definition 3 (Closed Euclidean ball (ball))**.** *Define the Euclidean ball centred at $\boldsymbol{p} \in \mathbb{R}^3$ with radius r (henceforth just "ball", for brevity) as:*

$$\mathcal{B}(\boldsymbol{p}\,;r) = \{\boldsymbol{x} \mid \|\boldsymbol{x} - \boldsymbol{p}\| \leq r\}$$

Let $\overline{\boldsymbol{p}_a, \boldsymbol{p}_b}$ denote the line segment between (and including) $\boldsymbol{p}_a$ and $\boldsymbol{p}_b$. We also define the Minkowski sum of two sets:

Definition 4 (Minkowski Sum)**.** *The Minkowski sum ($\oplus$) of set A and set B is defined as:*

$$A \oplus B = \{a + b \mid a \in A, b \in B\}$$

We can now formally define a capsule:

Definition 5 (Capsule)**.** *A capsule $\mathcal{C}$ with defining points $\boldsymbol{p}_a$ and $\boldsymbol{p}_b$, and radius r, is defined as:*

$$\mathcal{C} = \overline{\boldsymbol{p}_a, \boldsymbol{p}_b} \oplus \mathcal{B}(\boldsymbol{0}\,;r)$$

We now introduce two operators, CE and BE, which enclose two balls in a minimum-volume capsule, and in a minimum-volume ball, respectively. Consider the balls $\mathcal{B}(\boldsymbol{p}_1;r_1)$ and $\mathcal{B}(\boldsymbol{p}_2;r_2)$. Let us define:

$$\iota = \mathtt{indmax}(r_1, r_2), \qquad \kappa = \mathtt{indmin}(r_1, r_2)$$
$$\boldsymbol{x} = \boldsymbol{p}_\iota - \boldsymbol{p}_\kappa, \qquad \alpha = \max(r_\iota - r_\kappa, \|\boldsymbol{x}\|) \tag{7}$$
$$\beta = \min(r_\iota - r_\kappa, \|\boldsymbol{x}\|) \qquad \boldsymbol{p}_3 = \boldsymbol{p}_\kappa + \frac{\beta\boldsymbol{x}}{\|\boldsymbol{x}\|}$$

The operators $\mathtt{indmin}$ and $\mathtt{indmax}$ give the indices of the minimum and maximum of their arguments. Let $\boldsymbol{0} \in \mathbb{R}^3$ be the vector of zeros. We can then define the operators:

$$\mathtt{CE}(\mathcal{B}(\boldsymbol{p}_1;r_1), \mathcal{B}(\boldsymbol{p}_2;r_2)) := \overline{\boldsymbol{p}_\iota, \boldsymbol{p}_3} \oplus \mathcal{B}(\boldsymbol{0}\,;r_\iota),$$
$$\mathtt{BE}(\mathcal{B}(\boldsymbol{p}_1;r_1), \mathcal{B}(\boldsymbol{p}_2;r_2)) := B\left(\frac{\boldsymbol{p}_\iota + \boldsymbol{p}_3}{2}; \frac{r_\iota + r_\kappa + \alpha}{2}\right). \tag{8}$$

The operators BE and CE give the enclosing ball and capsule with minimal volume; this is shown in Appendix A.

B. Robot Occupancy

We enclose the robot's geometry in a set of capsules $\mathcal{U}$, see Fig. 3(a). Recall the definition of a trajectory in Def. 1 as a function in joint space parameterised by a time parameter s. Our algorithm yields capsules $\mathcal{C}_i$, which enclose the robot's
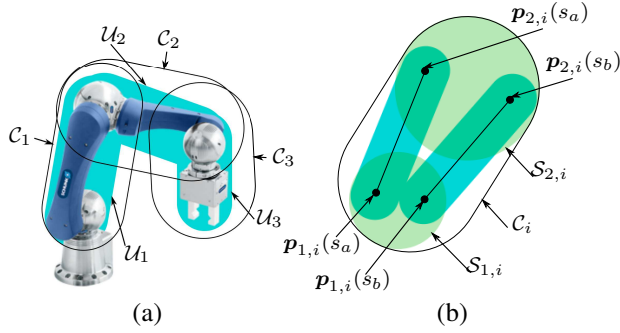
Fig. 3. (a) the geometry of the robot's i^{th} link enclosed in a capsule $\mathcal{U}_i$ (b) each link's occupancy over the short-term plan enclosed in a capsule $\mathcal{C}_i$.
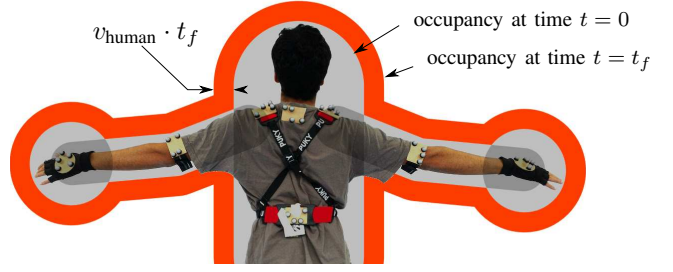

Fig. 4. The occupancy of the human, at the time of sensing ($t = 0$) and at future time t_f. The positions of the spheres and capsules used for defining the occupancy are determined from the positions of markers on the hands, elbows, shoulders, and the neck (the marker on the back is not used).

geometry over the section of path from the start s_a to the end s_b of the short-term plan; these are the black outlined capsules in Fig. 3. Fig. 3(a) shows how the robot reachable occupancy (RRO) is the union of these capsules; Fig. 3(b) shows how each capsule $\mathcal{C}_i$ is calculated.

We perform the computation link by link. Let the Cartesian positions of the defining points of the ith capsule $\mathcal{U}_i$ in the global frame be $\boldsymbol{p}_{1,i}$ and $\boldsymbol{p}_{2,i}$. These can be found from forward kinematics, i.e. $\boldsymbol{p}_{1,i}$ and $\boldsymbol{p}_{2,i}$ are functions of joint position. Since joint position is in turn a function of path parameter s, we express the Cartesian positions of the defining points of capsule i as $\boldsymbol{p}_{1,i}(s)$ and $\boldsymbol{p}_{2,i}(s)$. To obtain the capsule $\mathcal{C}_i$ enclosing the capsule $\mathcal{U}_i$ as it moves from s_a to s_b, we calculate first the balls $\mathcal{S}_{1,i}$ and $\mathcal{S}_{2,i}$, which enclose the path in space of defining points $\boldsymbol{p}_{1,i}(s)$ and $\boldsymbol{p}_{2,i}(s)$ of $\mathcal{U}_i$ as they move from s_a to s_b, and enlarge this by the radius of $\mathcal{U}_i$, $r_{\mathcal{U}_i}$:

$$\mathcal{S}_{1,i} \supseteq \{\boldsymbol{p}_{1,i}(s)|s \in [s_a, s_b]\} \oplus \mathcal{B}(0; r_{\mathcal{U}_i}),$$
$$\mathcal{S}_{2,i} \supseteq \{\boldsymbol{p}_{2,i}(s)|s \in [s_a, s_b]\} \oplus \mathcal{B}(0; r_{\mathcal{U}_i}).$$

Enclosing the paths from $\boldsymbol{p}_{1,i}(s_a)$ to $\boldsymbol{p}_{1,i}(s_b)$ and from $\boldsymbol{p}_{2,i}(s_a)$ to $\boldsymbol{p}_{2,i}(s_b)$ is not trivial. However, we can approximate the paths as straight lines and upper bound the deviation from the lines. Let the upper bounds of $\left\|\frac{\mathrm{d}^2\boldsymbol{p}_{1,i}(s)}{\mathrm{d}s^2}\right\|$ and $\left\|\frac{\mathrm{d}^2\boldsymbol{p}_{2,i}(s)}{\mathrm{d}s^2}\right\|$ for $s \in [s_a, s_b]$ be called $\alpha_{1,i}$ and $\alpha_{2,i}$ respectively. Since the nominal trajectory is always known prior to the computation of the short-term plan, the values $\alpha_{1,i}$ and $\alpha_{2,i}$ can be computed in advance. From [7, Thm. 2], these deviations of $\boldsymbol{p}_{1,i}$ and $\boldsymbol{p}_{2,i}$ are maximally $\alpha_{1,i}\frac{(s_a-s_b)^2}{8}$ and $\alpha_{2,i}\frac{(s_a-s_b)^2}{8}$ respectively. Hence:

$$r_{1,i} = \alpha_{1,i}\frac{(s_a-s_b)^2}{8} + r_{\mathcal{U}_i}, \quad r_{2,i} = \alpha_{2,i}\frac{(s_a-s_b)^2}{8} + r_{\mathcal{U}_i},$$
$$\mathcal{S}_{1,i} = \text{BE}(\mathcal{B}(\boldsymbol{p}_{1,i}(s_a); r_{1,i}) \, , \, \mathcal{B}(\boldsymbol{p}_{1,i}(s_b); r_{1,i}))$$
$$\mathcal{S}_{2,i} = \text{BE}(\mathcal{B}(\boldsymbol{p}_{2,i}(s_a); r_{2,i}) \, , \, \mathcal{B}(\boldsymbol{p}_{2,i}(s_b); r_{2,i}))$$
$$\tag{9}$$

Balls $\mathcal{S}_{1,i}$ and $\mathcal{S}_{2,i}$ are enclosed in a capsule to obtain $\mathcal{C}_i$:

$$\mathcal{C}_i = \text{CE}(\mathcal{S}_{1,i}, \mathcal{S}_{2,i})$$

If the short-term plan is long, the overapproximation may be large. In this case, we may subdivide the section of path from s_a to s_b, and take the occupancy as the union of the volumes calculated for each subdivision.

C. Human Occupancy

In previous work, we showed how the human occupancy could be determined as a union of sphere-swept volumes, based on maximum acceleration and speeds determined from motion capture of extreme movements [39]. However, for a fair comparison with the SRMS method, we assume only a maximum speed for the human of $v_{\text{human}} = 2.0\frac{m}{s}$, as used in Sec. IV-B, eq. (10), and no further assumptions.

The instantaneous occupancy of the human is modelled as two spheres enclosing the hands, and five capsules enclosing the two lower arms, two upper arms, and the torso and head together. These are defined using the positions of retroreflective markers on the hands, elbows, shoulders, and neck as seen in Fig. 4, tracked by a 6-camera Vicon Vero 1.3 system, and include position uncertainty.

The occupancy at a future point in time $t = t_f$ from an observation at time $t = 0$ is simply the occupancy at $t = 0$ with the radii of the capsules increased by $v_{\text{human}} \cdot t_f$, as shown in Fig. 4. Consequently, the occupancy during the time interval $[t_i, t_f]$ is equivalent to the occupancy at t_f only. The value of t_f is the stopping time of the robot (i.e. the end time of the short-term plan it is on). Note that t=0 is prior to the time of verification due to sensor, transmission, and software latency. In our setup, transmission latency was taken as $1ms$, control cycle time (of robot control including the safety layer) was $2ms$ and the sensor latency was $4ms$ (from the camera frame-rate of $250Hz$) plus software latency. The product website[2] gives a latency of $2.8ms$ for 10 objects. We had 7 objects, and we took the software latency conservatively to be $5ms$. This results in $12ms$, meaning the prediction horizon is the length of the short-term plan plus $12ms$.

IV. USER STUDY

As mentioned in the introduction, we compare two operation modes permitted in ISO 10218-1 [2]: safety-rated monitored stop (SRMS) and formally-verified speed and separation monitoring (VSSM) using our novel approach, both implemented

---

[2]www.vicon.com/products/software/tracker, retrieved: 26.12.2017
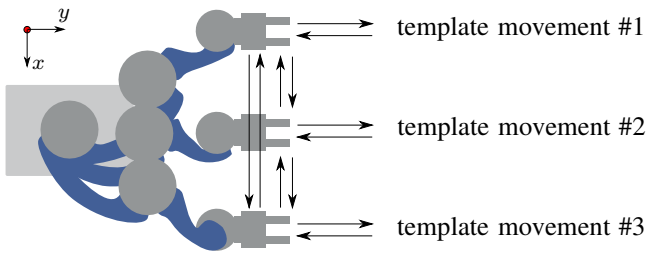
Fig. 5. Desired trajectory: away from the base in the y-direction for $1.7s$, back for $1.7s$. The robot moves randomly between three different starting positions.

Fig. 6. Workspace simulation with human, robot, workbench, and virtual cage (red) enclosing the robot workspace.

in accordance with ISO 10218-1 [2] and ISO 13855 [40]. We only planned recovery manoeuvres to $\eta = 1$ in this implementation of VSSM.

Below, we present the desired trajectory of the robot used in our experiments, followed by our implementation of the control condition, SRMS. We then describe the experimental procedure, the questionnaires used, and finally our hypotheses.

A. Robot nominal trajectory

The robot's desired trajectory is a series of predefined motions in randomised order. We chose these motions since they did not represent a task that the user could associate with any level of danger (or safety), were randomised so that the user could not predict a pattern and use that pattern to avoid the robot, and there was no possibility of clamping. The robot first moves to a start position, moves outward ($10cm$ in the y-direction) for $1.7s$, and $15cm$ inward again for $1.7s$. It then either moves to a new location on the x-axis or stays in the same location (a movement of between 5 and $60cm$). Afterwards, the robot repeats the outward-inward movement. There are 3 different x-axis locations, shown in Fig. 5, and the robot chooses the location for its next outward-inward movement at random and with equal probability. It does this continually until the human finishes their task. The maximum velocity of the tool centre point is $0.43\frac{m}{s}$. The maximum allowed joint accelerations $\boldsymbol{a}_m$ and jerk $\boldsymbol{j}_m$ were $10rad/s^2$ and $200rad/s^3$ for all joints.

The movements of the tool centre point are piecewise straight-line and limited-jerk in the Cartesian space (i.e., nominal distance along each straight-line piece of the trajectory is a quintic polynomial in time). In [41], it is observed that straight-line movements are better for human performance and well-being, possibly due to their better predictability. Huber *et al.* [42] observed that straight lines with minimum-jerk velocity profiles led to more fluent handovers, compared to joint space point-to-point motions with trapezoidal, i.e. non-jerk-limited, velocity profiles.

B. Safety-rated monitored stop

The SRMS was implemented as a virtual cage: The workspace of the robot was enclosed in an axis-aligned bounding box as shown in Fig. 6. This was extended by the safety distance S as defined in [40, eq. 2], calculated as:
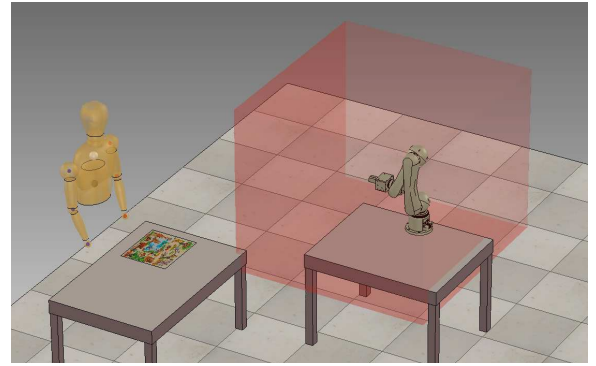
$$S = (K \cdot T) + C, \tag{10}$$

where the terms are defined as follows:

1) S: the safety distance.
2) K: the maximum speed of the human, $v_{\text{human}} = 2.0\frac{m}{s}$.
3) T: the lag of the entire sensing loop, i.e. the sensor and transmission latency, control cycle time and robot stopping time. The stopping time was taken as the maximum over the trajectory: $174ms$. The rest was taken as $12ms$ as in Sec. III-C. Together, this gave $T = 186ms$.
4) C: penetration distance: the amount that the human can penetrate the co-working area without being detected, relevant for light curtains with a beam resolution. For us, this is irrelevant, since we use infrared motion capture.

This yields $S = 0.372m$. If any marker on the human enters the cage, the robot performs a stop identical to the failsafe manoeuvre of the VSSM approach described previously.

C. Experimental Procedure

Subjects were healthy, aged between 22 and 30 years old, 13 male and 15 female. Each experiment had two experimenters: one to interact with the subject, the other to operate the robot. Subjects were assigned at random to VSSM or SRMS, and the first experimenter was not made aware of which condition was assigned. Subjects did not see or interact with any other subjects in the lab. We had 15 subjects in the VSSM group and 13 subjects in the SRMS group. The robot used for this study was a 6-degree-of-freedom Schunk LWA 4P with a Schunk 2-finger parallel gripper, running in position control at 500Hz.

Subjects were first informed about the purpose and procedure of the study, signed a declaration of consent, and completed questionnaires F0 and F1. They then watched an instruction video of their task, and the instructor answered questions pertaining to this (but not the robot or its task), and attached tracking markers to the subject. The subject's task was to assemble a children's jigsaw puzzle (Fig. 7(a)) on a table outside the robot's workspace. The pieces for the puzzle were in the robot workspace, arranged as shown in Fig. 7(b) at the robot base. To complete the puzzle, the subject had to enter the workspace of the robot and pick one piece at a time, return to the table, and fit the piece in the puzzle, see Fig. 8.

Subjects practiced the puzzle task once without the robot moving; this was not timed. They then performed their task
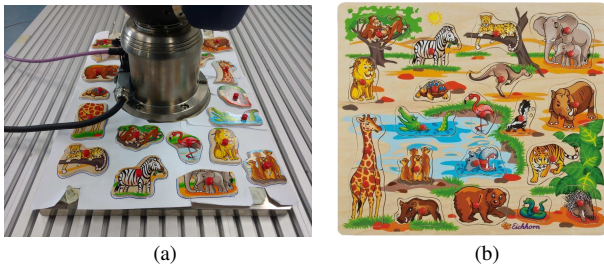
Fig. 7. (a) The pieces in position at the robot base, (b) the completed puzzle.
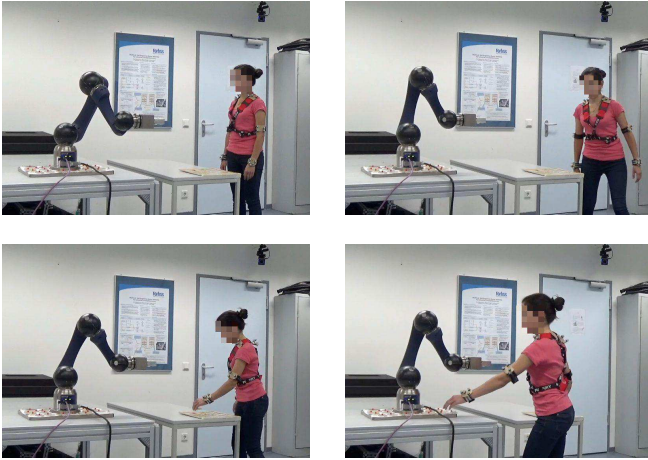

Fig. 8. The human's task: starting at their workbench (top left), the human approaches (top right) to pick a puzzle piece from the robot base (bottom right), and place it in the puzzle at their workbench (bottom left). They repeat this piece-by-piece until the puzzle is completed.

simultaneously with the robot performing its task. Following this first trial, they completed questionnaire F2, then performed another 3 trials with the same setup. At the second and third appointments, 4 trials were conducted. After the last trial, questionnaires F3 and F4 were completed.

D. Hypotheses

Hypotheses 1-4 pertained to *efficiency* and were tested by timing the activity. Human time to completion (TTC) was measured with a stopwatch; robot idle time was defined as the nominal planned time of completed robot movements (i.e. if there had been no slowing/stopping due to humans in the workspace) subtracted from the actual time the robot took. Hypotheses 5-12 pertained to human factors, and were tested via the questionnaires described in Appendix B.

Efficiency hypotheses

H1 VSSM leads to less robot idle time than SRMS;
H2 VSSM leads to different human TTC than SRMS;
H3 Robot idle time decreases with number of trials, for (a) VSSM and (b) SRMS;
H4 Human TTC decreases with number of trials, for (a) VSSM and (b) SRMS.

Human factors hypotheses

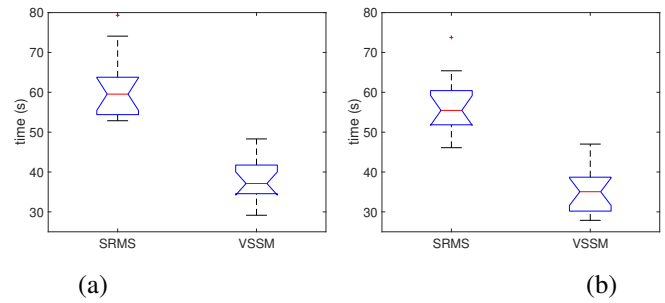For VSSM (a) and SRMS (b), subjects:

Fig. 9. Box-and-whisker plots showing average robot idle times in (a) the first 4 trials, (b) the last 4 trials.

H5 have different *propensity to trust* the system after multiple trials;
H6 feel different *satisfaction* with the robot as a co-worker after multiple trials;
H7 feel different *comfort* after multiple trials;
H8 have different impressions of the *intention of the developers* after multiple trials;
H9 have different *understanding* of the robot's movement after multiple trials;
H10 have different *perception of safety* of the robot after multiple trials.

After one trial (a) / after 12 trials (b) with the robot, subjects:

H11 have different *perception of safety* with SRMS than VSSM;
H12 have different *understanding* of the robot's movement with SRMS than VSSM.

V. EXPERIMENTAL RESULTS

Robot idle time was 36% less in VSSM than in SRMS, averaged over all trials. With increasing numbers of trials, both human TTC and robot idle time decreased. Of the human factors hypotheses, only perception of safety was seen to improve in both groups after 12 trials, though understanding improved in the VSSM group. We describe the results in detail.

A. Efficiency hypotheses

For each subject, we found the mean human TTC and robot idle time over a) the four trials on the first day, b) the four trials on the last day, and c) all trials. We tested this data for normality using the Shapiro-Wilk test [43]. In the SRMS group the robot idle times on the first day and the human TTC on the last day were significantly non-normally distributed ($p < 0.05$ when data is normally distributed), so to test hypotheses H1 and H2 we used the Kruskal-Wallis H-test [44] [3] and the median instead of the mean as an average.

H1: The median[4] robot idle time in the VSSM group is 38% lower than that of the SRMS group ($p < 10^{-5}$) over the first 4 trials and 37% ($p < 10^{-5}$) over the last 4 trials, showing that

---

[3]Kruskal-Wallis H-test does not require normally distributed data; it is the non-parametric equivalent to the more usual analysis of variance (ANOVA).

[4]We use the median since the tests were non-parametric. For each person, their mean TTC and robot idle time was found for each day of trials; for both groups, the median of these mean times was used to compare.
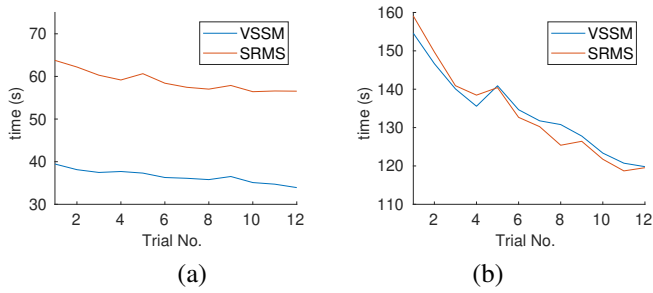
Fig. 10. How (a) median robot idle time, (b) the median human TTC developed over the trials.

TABLE I
IDLE TIME FOR ROBOT AND TTC FOR HUMAN SUBJECT (SECONDS), MEDIAN AND INTERQUARTILE RANGE

	Robot idle time				Human TTC			
	VSSM		SRMS		VSSM		SRMS	
Trial	med	IQR	med	IQR	med	IQR	med	IQR
1–4 avg.	37.1	7.2	59.5	9.4	146.6	31.4	148.1	35.5
5–8 avg.	36.6	8.6	55.0	10.6	137.0	32.5	123.1	26.8
9–12 avg.	35.1	8.5	55.5	8.6	124.2	43.6	117.0	21.0
avg. all trials	36.2	8.4	56.6	10.3	137.4	36.8	128.5	27.1

the efficiency advantage of VSSM persists even after training. The median value of each subjects time for all trials was 36% lower in VSSM than SRMS ($p < 10^{-5}$). The times are shown in Tab. I and in box plots in Fig. 9.

H2: no significant difference was found in human TTC, neither on the first day, nor the last day, nor over all trials.

H3 and H4 test the accustomisation of the human to the robot. The distribution of the mean TTC and robot idle time for each subject were not significantly different to normal, hence repeated measures ANOVA were applied to the data.

H3: a decrease in robot idle time was observed in a) the VSSM group of 14% ($p < 10^{-4}$), and b) the SRMS group of 11% ($p < 10^{-4}$); see Fig. 10(a).

H4: a decrease in human TTC was observed in a) the VSSM group of 22% ($p < 10^{-6}$), and b) the SRMS group of 25% ($p < 10^{-6}$); see Fig. 10(b).

B. Human factors hypotheses

The human factors hypotheses are summarised in Tab. II. For hypotheses H5, H6 and H7, the scales used to measure propensity to trust, satisfaction and comfort were not internally consistent when tested using Cronbach's alpha [45].

For the remaining hypotheses, we checked whether the data was significantly different from normal using the Shapiro-Wilk test, using the non-parametric Kruskal-Wallis test between groups (or Friedman test [46] for repeated measures) if so and ANOVA (or repeated-measures ANOVA) if not.

TABLE II
SUMMARY OF RESULTS FOR HYPOTHESES

Hypo-thesis	Shapiro-Wilk p	Cronbach α	Test	p	Result
H5, H6, H7	-	< 0.6	-	-	not internally consistent
H8 (a)	-	0.69	-	-	insufficient data
H8 (b)	< 0.05	0.69	Friedman	0.0027	accept
H9 (a)	> 0.05	0.82*	ANOVA	0.0207	accept
H9 (b)	< 0.05	0.82*	Friedman	0.0833	reject
H10 (a)	> 0.05	0.75	ANOVA	0.0128	accept
H10 (b)	< 0.05	0.75	Friedman	0.0082	accept
H11 (a)	> 0.05	0.75	ANOVA	0.2778	reject
H11 (b)	< 0.05	0.75	Kruskal-Wallis	0.0100	accept
H12 (a)	> 0.05	0.82*	ANOVA	0.3358	reject
H12 (b)	< 0.05	0.82*	Kruskal-Wallis	0.1832	reject

* omitting item 19 "I was distracted by the robots movement."

For H6(a), 6 out of 15 answers were "no response preferred", so we did not evaluate this hypothesis due to missing data. H6(b) showed a clear improvement in the trust in the intention of the developers after trials. H7 showed a significant improvement in understanding in VSSM; the improvement was not significant in SRMS ($p = 0.0833$), however, this may have been due to a small effect size. If more subjects had been used, perhaps significance at the 5% level may have been observed. H10(a) and (b) could be accepted: perception of safety improves in both the VSSM and SRMS groups after 12 trials compared to after 1 trial.

No significant difference in understanding was found between the groups (H12) either at the beginning nor at the end of the experiment. A difference in perceived safety (H11) was, however: subjects in the SRMS group had higher perceived safety after all trials than the VSSM group; no significant difference was found after only one trial.

The last four questions of F4, concerning the attitude of the subject towards the robot waiting and their self-assessment of how they adapted to the robot, are shown in Fig. 11.

VI. DISCUSSION

The increased efficiency in VSSM can be explained since the robot must only alter its behaviour if the human is in danger of collision, while in SRMS the robot stops as soon as the human enters its workspace. A subject (from the VSSM group) also commented that if they saw the robot moving to one side they would try to take puzzle pieces from the other side. This adaptation to the robot's behaviour would improve efficiency in VSSM, but not in SRMS, where the robot would stop regardless of where the human is in its workspace. Since
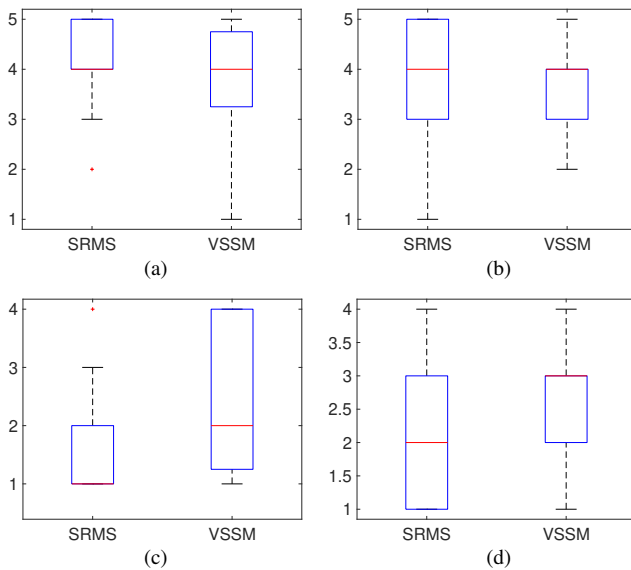
Fig. 11. Box plots of responses to questions of F4: (a) "I understand how the robot works better than at the start."; (b) "I feel safer, when the robot waits for me."; (c) "I need more time to adapt to the behaviour of the robot."; (d) "It is annoying when the robot waits for me. " for SRMS (left) and VSSM (right). 1 is "strongly disagree" and 5 is "strongly agree".

subjects get faster at the task with practice, both human TTC and robot idle time decrease over time.

A. Perceived safety

In the first appointment (after the first trial) there was no significant difference in perceived safety, however, after 12 trials, perceived safety in the SRMS group was significantly higher than VSSM. This seems to justify the use of longer trials since distinct effects can be observed after the novelty of a system has worn off. It also appears to back up the findings of [12], where separate workspaces increased perceived safety during tests in VR.

An explanation could be that in SRMS, the robot stopped earlier and further away from the human than VSSM. In [47] it is observed that keeping distance even beyond the necessary safe distance increases subjects' safety and comfort. However, several factors, including personality, determine how close the robot can come for the user's comfort [48], [49].

Important to note is that perceived safety is significantly higher after exposure to the robot with *both* approaches. In the VSSM group, 6 out of 15 agreed that they need more time to adapt to the behaviour of the robot, compared to 1 out of 13 in the SRMS group, though most still agreed that they understood how the robot works better than at the start (see Fig. 11). It could therefore be the case that subjects just require more training to feel completely safe with VSSM.

B. Attitudes towards the robot

Only one subject in each group "rather agreed" with the statement "It is annoying when the robot waits for me", and only three subjects in the whole study disagreed with "I feel safer, when the robot waits for me". The majority in both

groups felt safer, and not annoyed, when the robot waited for them. In [26], the human could either go first or yield to the robot, when workspace conflicts prevented simultaneous working. The authors concluded that subjects prefer to make the robot wait for them, on the basis that the robot was idle for longer than the human. Among other reasons, humans may prefer to be the dominant partner in the interaction and make the robot wait: humans have been found to have greater trust in a less dominant robot [50].

C. Understanding of the robot

Understanding of the robot's movement increased between the first and the last trial for our method (i.e. VSSM). This is shown in Tab. II (hypothesis H9(b)), and also in Fig. 11(a). There was no significant increase of understanding in the control method (i.e. SRMS), however, as mentioned in Sec. V-B, if more subjects had been used, significance at the $p < 0.05$ level might have been observed. Furthermore, both at the start and at the end, there was no significant difference in understanding between the methods (Tab. II, hypothesis H12). Thus, we cannot comment on the differences between the methods.

Most subjects began to understand that the robot reacted to their proximity. One subject (from the VSSM group) believed that the robot, when recovering back to its original trajectory, would go faster to try to make up lost time; another believed that the robot adapted to them over time, and was surprised to hear this was not the case. A further subject noted that the robot could improve its efficiency by learning and recognising the human's movements so as to avoid them.

D. Elements differing from a factory environment

Differences between this setup and a factory environment may affect perceived safety and trust in the developers.

1) Differences in setup: Firstly, the harmonic drives on the robot were loud. On one hand, an advantage of experiments with a physical robot (as opposed to with video recordings) is that the robot's noise and vibrations are impossible to ignore. On the other hand, one subject said they used the noise to tell when the robot was moving without looking; this would be impossible wearing ear defenders on a noisy factory floor.

A retroreflective marker-based system that the user must wear is also not representative of sensing used in a factory environment. Camera-based systems may be used, e.g. the Pilz SafetyEYE[5]; these are less intrusive, but also less visible to the user. A visual or audible signal when tracking is on, or a screen displaying the tracked representation of the user, could be reassuring and make the user feel safer.

2) Robot Physiognomy: Secondly, the robot is fairly small (though typical for a co-bot) and has 6 DOFs. The movement of a redundant (>6-DOF) robot—even in straight lines—may be more difficult to predict and thus unsettling for the user. The use of a larger, high-inertia robot may also affect perception of safety. One subject observed that they would have taken more care had the robot been faster or the end-effector sharp, hazardous or undesirable to touch, like a marker pen.

[5]pilz.com/de-DE/eshop/00106002207042/SafetyEYE-Sicheres-Kamerasystem, retrieved 11.12.20

3) Robot Movement: The robot's task was a set of straight-line movements. In a factory, workers' training would include information on what nearby robots are doing, to various levels of detail. The amount and depth of training is another factor that will affect the workers' understanding, and hence perception of safety, of the robot. The presence of pinch-points or clamping hazards, which might occur in a real setting, would make the robot more hazardous.

Early on in the trials, the low-level control of the robot stopped working due to a mechanical fault (not during any trials used in this study). While correcting this problem, we had to reschedule appointments; though we did not tell the affected subjects why their appointment was rescheduled, this could have nevertheless impacted their trust in the system.

The instruction video told subjects to work quickly but without rushing. There seemed to be a difference in how this was interpreted, however, the investigators did not interfere to hurry up slow workers, so as not to influence natural behaviour when interacting with the robot. In a time-bound production environment, this would not be the case. Finally, choosing lower allowable maximum accelerations/jerks for the failsafe manoeuvre would make 1) the failsafe manoeuvre longer and cause the robot to start slowing earlier when the human approaches and 2) the movement smoother during a failsafe manoeuvre. This may seem less threatening to the user.

E. Attitudes towards the developers and sympathy/antipathy towards automation

The more positive attitude towards the developers and their intentions observed at the end of trials for the control method (i.e. SRMS, hypothesis H8(b)) could be because subjects associated the developers with those carrying out the user study; as they got to know them over the course of the trials, they got to trust them. This would not be the case in a factory environment, where those working with the robot might never associate the responsibility for the robot's operation with a human being they can trust. A crucial difference to studies with factory workers is the robot has no impact in the lives of user-study participants, but may be perceived to impact the job and employment prospects of factory workers, affecting workers' acceptance and therefore trust in the technology [51].

F. Limitations of VSSM

Our tests were with accurate, low-latency sensing. Where sensor latency is higher (over tens of milliseconds), the reachable occupancy of the human must be enlarged by the amount of latency and the movement of the robot is more conservative. This is a generic limitation of SSM; where sensor latency is too high, other modes of co-working, e.g. power and force limiting, should be considered.

The current method neither learns from human motion, nor replans the desired trajectory—both useful if the robot is continually blocked by repetitive, easily predictable movements of the human. Learning methods can be integrated into VSSM by modifying the desired trajectory of the robot, as in e.g. [52].

Finally, the human co-worker did not have much insight into the robot motion. If coupled with visual cues (e.g.
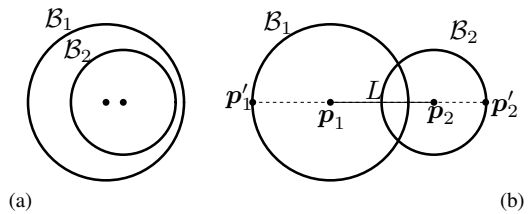

Fig. 12. Cases (a) and (b) in Thm. 1. Note: in (b), spheres might not overlap.

lights/display showing when the robot is slowing its motion in response to the worker) understanding could be improved.

VII. CONCLUSION AND FURTHER WORK

This paper presents an approach to formally-verified speed and separation monitoring in human-robot co-working, and compares it in a user study with an approach based on static safety zones. Not only the efficiency of the approaches is compared, but we examine, compare and discuss the human factors aspects of the approaches. Our study sheds light on what humans perceive as safe in human-robot co-working and should pave the way for more in-depth comparative studies into operating modalities for human-robot coexistence.

Above all, this study does not only report subject's first impressions of the robot but also their impressions after working for some time. This provides a more balanced picture of human-robot coexistence, since humans in a factory setting will work with robots over longer periods of time.

A drawback of studies at research institutions is that subjects are often drawn from institution staff and students, whose attitudes towards technology may be different to production line workers, despite the fact we recruited only subjects with little or no experience of robots. One promising research trend (e.g. [53]–[55]) is human-robot coexistence studies in factory environments with a more representative demographic.

APPENDIX A
PROOFS OF MINIMAL VOLUME ENCLOSURE

Theorem 1. *The operator* BE *yields a ball of least volume that encloses* $\mathcal{B}_1 = \mathcal{B}(\boldsymbol{p}_1; r_1)$ *and* $\mathcal{B}_2 = \mathcal{B}(\boldsymbol{p}_2; r_2)$.

Proof. Let $r_1 \geq r_2$, without loss of generality. Consider cases (a) $\mathcal{B}_2 \subseteq \mathcal{B}_1$ and (b) $\mathcal{B}_2 \nsubseteq \mathcal{B}_1$, shown in Fig. 12. For case (a), $\mathrm{BE}(\mathcal{B}_1, \mathcal{B}_2) = \mathcal{B}_1$. For case (b), we have from (7) that $\alpha = \|\boldsymbol{x}\| = \|\boldsymbol{p}_1 - \boldsymbol{p}_2\|$. Let L be the line defined by $\boldsymbol{p}_1$ and $\boldsymbol{p}_2$, and points $\boldsymbol{p}'_1$ and $\boldsymbol{p}'_2$ be the intersection of L and the boundaries of $\mathcal{B}_1$ and of $\mathcal{B}_2$, as in Fig. 12. Since the enclosing ball must contain both $\boldsymbol{p}'_1$ and $\boldsymbol{p}'_2$, its diameter is at least $\|\boldsymbol{p}'_1 - \boldsymbol{p}'_2\| = r_1 + r_2 + \|\boldsymbol{p}_1 - \boldsymbol{p}_2\|$, which is the diameter of the ball given by $\mathrm{BE}(\mathcal{B}_1, \mathcal{B}_2)$ in (8) using $\alpha = \|\boldsymbol{x}\| = \|\boldsymbol{p}_1 - \boldsymbol{p}_2\|$. $\qquad\square$

Lemma 1. *A sphere* $\mathcal{S}$ *of radius* ρ_s *can be fully enclosed in a capsule* $\mathcal{C}$ *of radius* ρ_c *if and only if* $\rho_c \geq \rho_s$.

Proof. Let the defining points of $\mathcal{C}$ be $\boldsymbol{p}_a$ and $\boldsymbol{p}_b$, and the centre of $\mathcal{S}$ be $\boldsymbol{p}_s$. Sufficiency is easily demonstrated by choosing $\boldsymbol{p}_s \in \overline{\boldsymbol{p}_a, \boldsymbol{p}_b}$. Necessity is shown by defining the intersection points $\hat{\boldsymbol{p}}_1$ and $\hat{\boldsymbol{p}}_2$ of the sphere with a line which
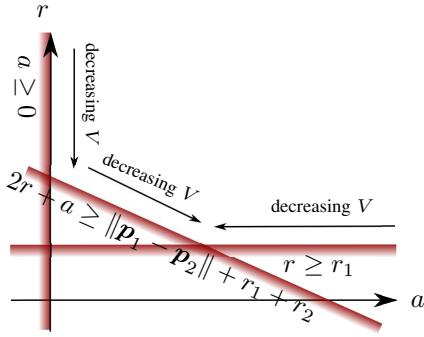
Fig. 13. Constrained optimisation problem from proof of Thm. 2. V has no minimum in the open upper-right quadrant; along the boundaries the V increases or decreases strictly monotonically, as long as $r \geq r_1$.

goes through its center and is perpendicular to $\overline{\boldsymbol{p}_a\,\boldsymbol{p}_b}$. Since the maximum distance of a point in the capsule to the line $\overline{\boldsymbol{p}_a\,\boldsymbol{p}_b}$ is ρ_c, the points $\hat{\boldsymbol{p}}_1$ and $\hat{\boldsymbol{p}}_2$ can only be enclosed if $\rho_c \geq \rho_s$. □

Lemma 2. *Consider a capsule $\mathcal{C}$ with defining points $\boldsymbol{p}_a$ and $\boldsymbol{p}_b$, and radius r, and arbitrary points $\boldsymbol{p}_x, \boldsymbol{p}_y \in \mathcal{C}$. Then $\|\boldsymbol{p}_x - \boldsymbol{p}_y\| \leq 2r + \|\boldsymbol{p}_a - \boldsymbol{p}_b\|$*

Proof. The distance of the point furthest away from the center is $r + 0.5\|\boldsymbol{p}_x - \boldsymbol{p}_y\|$. Thus, the maximum distance between two points in a capsule is at most twice that distance. □

Theorem 2. *The operator* CE *yields a capsule of least volume which encloses $\mathcal{B}_1 = \mathcal{B}(\boldsymbol{p}_1; r_1)$ and $\mathcal{B}_2 = \mathcal{B}(\boldsymbol{p}_2; r_2)$.*

Proof. Let $r_1 \geq r_2$, without loss of generality. Consider cases (a) $\mathcal{B}_2 \subseteq \mathcal{B}_1$ and (b) $\mathcal{B}_2 \nsubseteq \mathcal{B}_1$. For case (a), from the definitions in (7) and (8), $\mathtt{CE}(\mathcal{B}_1, \mathcal{B}_2) = \mathcal{B}_1$.

For case (b), we require to enclose $\mathcal{B}_1$ and $\mathcal{B}_2$ while minimising $\frac{4}{3}\pi r^3 + a\pi r^2$. Lem. 1 means the enclosing capsule's radius is $r \geq r_1$. Let the points $\boldsymbol{p}_1'$ and $\boldsymbol{p}_2'$ be defined as in the proof of Thm. 1 (see Fig. 12(b)). The magnitude of the distance between the defining points of the enclosing capsule is denoted by a. Both $\boldsymbol{p}_1'$ and $\boldsymbol{p}_2'$ must be contained in the enclosing capsule, so by Lem. 2, $\|\boldsymbol{p}_1' - \boldsymbol{p}_2'\| = \|\boldsymbol{p}_1 - \boldsymbol{p}_2\| + r_1 + r_2 \leq 2r + a$. We now have a bounded optimisation problem:

$$\text{minimise:} \quad V = \frac{4}{3}\pi r^3 + a\pi r^2$$

$$\text{subject to:} \quad r \geq r_1, \quad a \geq 0, \quad 2r + a \geq \|\boldsymbol{p}_1 - \boldsymbol{p}_2\| + r_1 + r_2$$

The partial derivatives of V are:

$$\frac{\partial V}{\partial r} = 4\pi r^2 + 2a\pi r, \qquad \frac{\partial V}{\partial a} = \pi r^2 \qquad (11)$$

In the open subspace $a, r > 0$, $\frac{\partial V}{\partial r}, \frac{\partial V}{\partial a} > 0$, so the minimum is on the boundaries. On these boundaries, V is monotonic as can be determined by (11) (see Fig. 13), except if $r_1 = 0$, in which case $\mathcal{B}_1$, $\mathcal{B}_2$ and the enclosing capsule have zero volume. Hence, the minimum is where lines $r = r_1$ and $2r + a = \|\boldsymbol{p}_1 - \boldsymbol{p}_2\| + r_1 + r_2$ intersect. One can verify that these r and a are those given by the algorithm of $\mathtt{CE}(\mathcal{B}_1, \mathcal{B}_2)$ as defined in (7) and (8) in Sec. III-A. □

APPENDIX B
QUESTIONNAIRES

The subjects completed 5 questionnaires during the experiment, F0-F4 (labelled in the order the subject takes them). F0 collected age, gender, and experience with robots. Only subjects with little or no experience with robots were used. F1 and F4 measured trust in the robot and feeling of safety, before and after trials. We used subquestionnaires *Propensity to Trust* (*PT*) and *Intentions of the Developers* (*ID*) from the questionnaire *Trust in Automation* in [56], where subjects rated their agreement with statements on a 5-point Likert scale. In F1 the questions referred to automated systems in general, and in F4, about our system in particular:

1 One should be careful with {unfamiliar automated systems / this system}, (*PT*)
2 I trust {a system/this system} more than I distrust it, (*PT*)
3 {Automated systems generally work/This system generally works} well, (*PT*)
4 The developers are trustworthy, (*ID*)
5 The developers take my well-being seriously, (*ID*)

In F4 we also added the questions 6-7 to gauge the subject's self-evaluation of their adaptation to the robot, and 8-9 to measure how the human feels about the robot waiting for them:

6 I understand how the robot works better than at the start,
7 I need more time to adapt to the behaviour of the robot,
8 I feel safer, when the robot waits for me,
9 It is annoying when the robot waits for me.

Questionnaires F2 and F3 had identical content (statements 10-20) and were administered after the first and the last trial, respectively. Statements 10-16 were taken from [26]. The authors of [26] classified items 10–12 as pertaining to the "satisfaction with the robot as a team-mate (*TM*)", and items 13–17 as pertaining to "perceived safety (*PS*) and comfort (*C*)". We also noticed that item 10 was also related to perceived safety in a human-robot coexistence scenario. We omitted their item: "The robot and I worked well together": the robot and human did not collaborate, so this question was irrelevant. We added statements 17-20, concerning how the subject was able to *understand* (*U*) how the robot moved.

10 I trusted the robot to do the right thing at the right time, (*TM/PS*)
11 The robot did not understand how I wanted to do the task, (*TM*)
12 The robot kept getting in my way, (*TM*)
13 I felt safe when working with the robot, (*PS*)
14 The robot moved too fast for my comfort, (*C*)
15 The robot came too close to me for my comfort, (*C*)
16 I trusted the robot would not harm me, (*PS*)
17 The reaction of the robot to me was easy to comprehend, (*U*)
18 The robots movement in my presence was confusing, (*U*)
19 I was distracted by the robots movement, (*U*)
20 The robots movement surprised me. (*U*)

REFERENCES

[1] T. Kopp, M. Baumgartner, and S. Kinkel, "Success factors for introducing industrial human-robot interaction in practice: an empirically driven framework," *The International Journal of Advanced Manufacturing Technology*, vol. 112, no. 3, pp. 685–704, 2021.

[2] "Robots and robotic devices - safety requirements for industrial robots - part 1: Robots," International Organization for Standardization, ISO Standard 10218-1:2011, 2011.

[3] J. Mainprice and D. Berenson, "Human-robot collaborative manipulation planning using early prediction of human motion," in *Proc. IEEE/RSJ Int. Conf. Intell. Rob. Sys.*, 2013, pp. 299–306.

[4] H. Ding, G. Reißig, K. Wijaya, D. Bortot, K. Bengler, and O. Stursberg, "Human arm motion modeling and long-term prediction for safe and efficient human-robot-interaction," in *Proc. IEEE Int. Conf. Robotics and Autom.*, 2011, pp. 5875–5880.

[5] J. Butepage, M. J. Black, D. Kragic, and H. Kjellstrom, "Deep representation learning for human motion prediction and classification," in *Proc. IEEE Conf. Comp. Vis. Pat. Recog.*, 2017, pp. 6158–6166.

[6] W. Mao, M. Liu, M. Salzmann, and H. Li, "Learning trajectory dependencies for human motion prediction," in *Proc. IEEE Int. Conf. Comp. Vision*, 2019.

[7] D. Beckert, A. Pereira, and M. Althoff, "Online verification of multiple safety criteria for a robot trajectory," in *Proc. IEEE Conf. Decision and Control*, 2017, pp. 6454–6461.

[8] S. Petti and T. Fraichard, "Safe motion planning in dynamic environments," in *Proc. IEEE-RSJ Int. Conf. Intell. Robots and Systems*, 2005, pp. 2210–2215.

[9] P. A. Lasota, T. Fong, and J. A. Shah, "A survey of methods for safe human-robot interaction," *Foundations and Trends in Robotics*, vol. 5, no. 4, pp. 261–349, 2017.

[10] N. Akalin, A. Kristoffersson, and A. Loutfi, "Do you feel safe with your robot? Factors influencing perceived safety in human-robot interaction based on subjective and objective measures," *International journal of human-computer studies*, vol. 158, 2022, article no. 102744.

[11] T. Jensen, Y. Albayram, M. M. H. Khan, M. A. Al Fahim, R. Buck, and E. Coman, "The apple does fall far from the tree: User separation of a system from its developers in human-automation trust repair," in *Proc. Designing Interactive Systems Conf.*, 2019, pp. 1071–1082.

[12] S. You, J.-H. Kim, S. Lee, V. Kamat, and L. P. Robert, "Enhancing perceived safety in human-robot collaborative construction using immersive virtual environments," *Automation in Construction*, vol. 96, pp. 161–170, 2018.

[13] P. A. Hancock, D. R. Billings, K. E. Schaefer, J. Y. C. Chen, E. J. de Visser, and R. Parasuraman, "A meta-analysis of factors affecting trust in human-robot interaction," *Human Factors*, vol. 53, no. 5, pp. 517–527, 2011.

[14] A. Rossi, K. Dautenhahn, K. L. Koay, and J. Saunders, "Investigating human perceptions of trust in robots for safe HRI in home environments," in *Proc. IEEE Int. Conf. Human-Robot Interaction*, 2017, pp. 375–376.

[15] D. De Siqueira Braga, M. Niemann, B. Hellingrath, and F. Buarque De Lima Neto, "Survey on computational trust and reputation models," *ACM Comput. Surv.*, vol. 51, no. 5, 2019.

[16] B. Sadrfaridpour and Y. Wang, "Collaborative assembly in hybrid manufacturing cells: An integrated framework for human-robot interaction," *IEEE Trans. Autom. Sci. Eng.*, vol. 15, no. 3, pp. 1178–1192, 2018.

[17] B. Sadrfaridpour, M. F. Mahani, Z. Liao, and Y. Wang, "Trust-Based Impedance Control Strategy for Human-Robot Cooperative Manipulation," in *Dynamic Systems and Control Conference*, vol. 1, 2018.

[18] M. Salem and K. Dautenhahn, "Evaluating trust and safety in HRI: Practical issues and ethical challenges," in *Proc. Workshop "Emerging Policy and Ethics of Human-Robot Interaction" at ACM/IEEE Int. Conf. Human Robot Interaction*, 2015.

[19] C. D. Kidd and C. Breazeal, "Robots at home: Understanding long-term human-robot interaction," in *Proc. IEEE/RSJ Int. Conf. Intell. Rob. Sys.*, 2008, pp. 3230–3235.

[20] I. Leite, C. Martinho, and A. Paiva, "Social robots for long-term interaction: A survey," *International Journal of Social Robotics*, vol. 5, no. 2, pp. 291–308, 2013.

[21] J. F. Hoorn, E. A. Konijn, D. M. Germans, S. Burger, and A. Munneke, "The in-between machine: The unique value proposition of a robot or why we are modelling the wrong things," in *Proc. Int. Conf on Agents and Artificial Intelligence*, 2015, pp. 464–469.

[22] A. C. Lo, P. D. Guarino, L. G. Richards, J. K. Haselkorn, G. F. Wittenberg, D. G. Federman, R. J. Ringer, T. H. Wagner, H. I. Krebs, B. T. Volpe, C. T. J. Bever, D. M. Bravata, P. W. Duncan, B. H. Corn, A. D. Maffucci, S. E. Nadeau, S. S. Conroy, J. M. Powell, G. D. Huang, and P. Peduzzi, "Robot-assisted therapy for long-term upper-limb impairment after stroke," *New England Journal of Medicine*, vol. 362, no. 19, pp. 1772–1783, 2010.

[23] J. D. van der Laan, A. Heino, and D. D. Waard, "A simple procedure for the assessment of acceptance of advanced transport telematics," *Transportation Research Part C: Emerging Technologies*, vol. 5, no. 1, pp. 1–10, 1997.

[24] M. Müllhäuser, "Tactile cueing with active cyclic stick for helicopter obstacle avoidance: development and pilot acceptance," *CEAS Aeronautical Journal*, vol. 9, no. 1, pp. 27–37, 2018.

[25] I. Gaudiello, E. Zibetti, S. Lefort, M. Chetouani, and S. Ivaldi, "Trust as indicator of robot functional and social acceptance. An experimental study on user conformation to iCub answers," *Computers in Human Behavior*, vol. 61, pp. 633 – 655, 2016.

[26] P. A. Lasota and J. A. Shah, "Analyzing the effects of human-aware motion planning on close-proximity human-robot collaboration," *Human Factors*, vol. 57, no. 1, pp. 21–33, 2015.

[27] S. Pellegrinelli, H. Admoni, S. Javdani, and S. Srinivasa, "Human-robot shared workspace collaboration via hindsight optimization," in *Proc. IEEE/RSJ Int. Conf. Intell. Rob. Sys.*, 2016, pp. 831–838.

[28] A. Dragan, R. Holladay, and S. Srinivasa, "An analysis of deceptive robot motion," in *Robotics: Science and Systems*, 2014, paper # 10.

[29] H. Knight, R. Thielstrom, and R. Simmons, "Expressive path shape (swagger): Simple features that illustrate a robot's attitude toward its goal in real time," in *Proc. IEEE/RSJ Int. Conf. Intell. Rob. Sys.*, 2016, pp. 1475–1482.

[30] K. L. Koay, D. S. Syrdal, M. L. Walters, and K. Dautenhahn, "Living with robots: Investigating the habituation effect in participants' preferences during a longitudinal human-robot interaction study," in *Proc. IEEE Int. Conf. Robot & Human Interactive Communication*, 2007, pp. 564–569.

[31] J. Reinhardt, A. Pereira, D. Beckert, and K. Bengler, "Dominance and movement cues of robot motion: A user study on trust and predictability," in *Proc. IEEE Sys. Man Cybernet.*, 2017, pp. 1493–1498.

[32] J. Lee and N. Moray, "Trust, control strategies and allocation of function in human-machine systems," *Ergonomics*, vol. 35, no. 10, pp. 1243–1270, 1992.

[33] M. Althoff, A. Giusti, S. B. Liu, and A. Pereira, "Effortless creation of safe robots from modules through self-programming and self-verification," *Science Robotics*, vol. 4, no. 31, pp. 1–14, 2019.

[34] J. Hollerbach, "Dynamic scaling of manipulator trajectories," *J. Dyn. Sys., Meas., Control*, vol. 106, no. 1, pp. 102–106, 1984.

[35] O. Dahl and L. Nielsen, "Torque-limited path following by online trajectory time scaling," *IEEE Trans. Robotics Autom.*, vol. 6, no. 5, pp. 554–561, 1990.

[36] R. Rossi, M. Polverini, A. Zanchettin, and P. Rocco, "A pre-collision control strategy for human-robot interaction based on dissipated energy in potential inelastic impacts," in *Proc. IEEE/RSJ Int. Conf. Intell. Rob. Sys.*, 2015, pp. 26–31.

[37] T. Kröger and F. Wahl, "Online trajectory generation: Basic concepts for instantaneous reactions to unforeseen events," *IEEE Trans. Robotics*, vol. 26, no. 1, pp. 94–111, 2010.

[38] H. Täubig, B. Bäuml, and U. Frese, "Real-time swept volume and distance computation for self collision detection," in *Proc. IEEE/RSJ Int. Conf. Intell. Rob. Sys*, 2011, pp. 1585–1592.

[39] A. Pereira and M. Althoff, "Overapproximative human arm occupancy prediction for collision avoidance," *IEEE Trans. Autom. Sci. Eng.*, vol. 15, no. 2, pp. 818–831, 2018.

[40] "Safety of machinery - positioning of safeguards with respect to the approach speeds of parts of the human body," International Organization for Standardization, ISO Standard 13855:2010, 2010.

[41] D. Bortot, M. Born, and K. Bengler, "Directly or on detours? How should industrial robots approximate humans?" in *Proc. ACM/IEEE Int. Conf. Human-Robot Interaction*, 2013, pp. 89–90.

[42] M. Huber, M. Rickert, A. Knoll, T. Brandt, and S. Glasauer, "Human-robot interaction in handing-over tasks," in *Proc. IEEE Int. Symp. Robot and Human Interactive Communication*, 2008, pp. 107–112.

[43] S. S. Shapiro and M. B. Wilk, "An analysis of variance test for normality (complete samples)," *Biometrika*, vol. 52, no. 3-4, pp. 591–611, 1965.

[44] W. H. Kruskal and W. A. Wallis, "Use of ranks in one-criterion variance analysis," *Journal of the American Statistical Association*, vol. 47, no. 260, pp. 583–621, 1952.

[45] L. J. Cronbach, "Coefficient alpha and the internal structure of tests," *Psychometrika*, vol. 16, no. 3, pp. 297–334, 1951.

[46] M. Friedman, "A comparison of alternative tests of significance for the problem of m rankings," *Ann. Math. Statist.*, no. 1, pp. 86–92, 1940.

[47] T. Kruse, A. K. Pandey, R. Alami, and A. Kirsch, "Human-aware robot navigation: A survey," *Robotics and Autonomous Systems*, vol. 61, no. 12, pp. 1726 – 1743, 2013.

[48] M. L. Walters, K. Dautenhahn, R. te Boekhorst, K. L. Koay, C. Kaouri, S. Woods, C. Nehaniv, D. Lee, and I. Werry, "The influence of subjects' personality traits on personal spatial zones in a human-robot interaction experiment," in *IEEE Int. Workshop on Robot and Human Interactive Communication.*, 2005, pp. 347–352.

[49] L. Takayama and C. Pantofaru, "Influences on proxemic behaviors in human-robot interaction," in *Proc. IEEE/RSJ Int. Conf. Intell. Rob. Sys*, 2009, pp. 5495–5502.

[50] J. Li, W. Ju, and C. Nass, "Observer perception of dominance and mirroring behavior in human-robot relationships," in *Proc. ACM/IEEE Int. Conf. Human-Robot Interaction*, 2015, pp. 133–140.

[51] A. Meissner, A. Trübswetter, A. S. Conti-Kufner, and J. Schmidtler, "Friend or foe? understanding assembly workers' acceptance of human-robot collaboration," *ACM Trans. Human-Robot Interaction*, vol. 10, no. 1, pp. 1–30, 2020.

[52] J. Thumm and M. Althoff, "Provably safe deep reinforcement learning for robotic manipulation in human environments," in *Proc. IEEE Int. Conf. Robotics and Autom.*, 2022.

[53] J. Kinugawa, Y. Kawaai, Y. Sugahara, and K. Kosuge, "PaDY: Human-friendly/cooperative working support robot for production site," in *Proc. IEEE/RSJ Int. Conf. Intell. Rob. Sys.*, 2010, pp. 5472–5479.

[54] S. Wrede, C. Emmerich, R. Grünberg, A. Nordmann, A. Swadzba, and J. Steil, "A user study on kinesthetic teaching of redundant robots in task and configuration space," *J. Human Robot Interaction*, vol. 2, no. 1, pp. 56–81, 2013.

[55] I. El Makrini, S. A. Elprama, J. Van den Bergh, B. Vanderborght, A.-J. Knevels, C. I. Jewell, F. Stals, G. De Coppel, I. Ravyse, J. Potargent, J. Berte, B. Diericx, T. Waegeman, and A. Jacobs, "Working with Walt: How a cobot was developed and inserted on an auto assembly line," *IEEE Robot. Autom. Mag.*, vol. 25, no. 2, pp. 51–58, 2018.

[56] M. Körber, E. Baseler, and K. Bengler, "Introduction matters: Manipulating trust in automation and reliance in automated driving," *Applied Ergonomics*, vol. 66, pp. 18–31, 2018.

Mareike Baumann is a Human Factors Consultant at the German Air Navigation Service Provider DFS. Since 2019, she holds a M.Sc. in Robotics, Cognition, Intelligence from the Technical University of Munich. Her current position involves the enabling of effective Human-Machine-Interaction in complex systems as well as working towards the strategic implementation of automation with the goal of a joint cognitive system.

Jonas Gerstner is a software engineer at robominds GmbH. He finished his M.Sc. in Robotics, Cognition, Intelligence at the Technical University of Munich in 2020. Currently, he is working on mobile kitting robots for challenging industrial environments.

Matthias Althoff is associate professor in computer science at Technische Universität München, Germany. He received his diploma engineering degree in Mechanical Engineering in 2005, and his Ph.D. degree in Electrical Engineering in 2010, both from the Technical University of Munich, Germany. From 2010 to 2012 he was a postdoctoral researcher at Carnegie Mellon University, Pittsburgh, USA, and from 2012 to 2013 an assistant professor at Technische Universität Ilmenau, Germany. His research interests include formal verification of continuous and hybrid systems, reachability analysis, planning algorithms, nonlinear control, automated vehicles, robotics, and power systems.

Aaron Pereira is a researcher at the Institute of Robotics and Mechatronics at the German Aerospace Centre (DLR), and a guest researcher at the Human Robot Interaction Lab of the European Space Agency. He received a Masters in Mechanical Engineering from Imperial College London in 2013 and a Ph.D. in safe human-robot co-existence from the Technical University of Munich in 2019. His recent research interest is in intuitive teleoperation, in particular for space applications.